

Diffusion-weighted MRI in the diagnosis of intracranial hematomas

Davut Şanlı, Özkan Ünal, Aydın Bora, Mehmet Beyazal, Alpaslan Yavuz, Serhat Avcu*

Department of Radiology, Yuzuncu Yil University Medical Faculty, Van, Türkiye

Abstract. To determinate the diagnostic value of diffusion-weighted MR imaging (DWI) in intracerebral hematomas, epidural hematomas, subdural hematomas, and subarachnoid hemorrhage, and to assess the contribution of diffusion signal characteristics in the differentiation of hematoma stages.

In this prospective study, consecutive 67 patients (range: 3-89 years), 35 (18 men 17 women) with intracerebral hematoma, 18 (10 men 8 women) with subdural hematoma, 2 (1 man 1 woman) with epidural hematoma, and 12 (5 men 7 women) with subarachnoid hemorrhage on conventional MRI sequences constituted the case group and were evaluated with DWI.

Intracerebral, subdural and epidural hematomas detected on conventional MR sequences were also shown on DWI. But none of the cases with subarachnoid hemorrhage was demonstrated on DWI.

All intracranial hematomas detected on DWI except from chronic stage subdural hematomas showed similar signal intensity characteristics on DWI and T2WI, but were hypointense on ADC maps.

All intracerebral, subdural and epidural hematomas seen on conventional MR sequences could be detected by DWI. On the contrary, DWI was not an effective imaging method for detecting subarachnoid hemorrhages.

Using DWI alone for detecting the stages of hemorrhages can provide only additional information in subdural and intracerebral hematomas, and it is unable to give definite results, and the lesions should be evaluated by the correlation with other conventional MRI sequences.

Key words: Diffusion weighted magnetic resonance imaging, intracranial hematomas

1. Introduction

Magnetic resonance imaging (MRI) has the highest soft tissue contrast resolution among all available radiological imaging modalities. Thus, it is widely used for imaging of all the soft tissues, especially central nervous system.

Recently newer MRI modalities are available together with other conventional MRI sequences. One of these modalities is diffusion-weighted imaging (DWI). DWI is a functional imaging technique which is based on the measurement of

alteration of microscopic diffusion movements in the protons of water molecules. Although DWI is mainly used in brain, it can be useful for detecting some other systemic diseases (1).

CT (Computerized Tomography) and MRI are used effectively for the detection of intracranial hematomas. MRI findings of different stages of hematomas are well established. MR signal intensity resulting from blood is mainly affected by several complicated factors such as hematocrit, oxygen content, tissue Ph, protein content of the clot, membrane stability of red blood cells, types of hemoglobin and chemical status of the iron that hemoglobin contains. Recently in addition to conventional MRI sequences, DWI has become an important imaging modality for detecting the stages of intracerebral hematomas. Several studies assessed the apparent diffusion coefficient (ADC) values of intracerebral hematomas according to their stages and reported that they have similar ADC values (2-6). Although there are some studies

*Correspondence: Serhat AVCU, MD, Associate Professor
Department of Radiology, Yüzüncü Yıl University Medical
Faculty, Van, Türkiye

Phone: +90 432 2150474

E-mail: serhatavcu@hotmail.com

Received: 16.04.2013

Accepted: 08.10.2013

which determine the ADC values of different stages of hematomas, data about the signal characteristics of different hematoma stages on DWI is very limited. Especially signal intensity characteristics of chronic hematoma is unclear and there is no an agreement between researchers for this stage. Findings of subdural hematoma on DWI are not clear (2-6).

As a result, in this study we aimed to search the diagnostic value of DWI for intracranial hematomas and to investigate signal characteristics of hematomas on DWI according to their stages.

2. Materials and Methods

A total of 67 patients (range 3-80 years) who were admitted to Radiology department between February 2010 to July 2010 were included in this prospective study. Informed consent was given to all patients and parents. Ethics committee approval has been obtained for the study.

Intracranial hematomas were classified into four groups: intracerebral hematoma, subdural hematoma, epidural hematoma, and subarachnoid hemorrhage. Case group was composed of 35 patients with intracerebral hematoma (18 male, 17 female), 18 patients with subdural hematoma (10 male, 8 female) 2 patients with epidural hematoma (1male, 1 female) and 12 patients with subarachnoid hemorrhage (5 male, 7 female) who were detected with conventional MRI sequences.

Intracerebral hematomas were classified into 5 stages according to their time of onset: hyperacute (0-12 hours, n:3), acute (13hours-3 days, n:5), early subacute (4-7 days, n:10) late

subacute (8-31 days, n:9) and chronic (more than 31 days, n:6).

Subdural hematomas were classified into 5 stages according to their time of onset: hyperacute (0-3 hours; n: 0), acute (3 hours-3 days; n: 2), early subacute (4-7 days; n: 4), late subacute (8 days-3 weeks; n: 8), and chronic (3 or more weeks; n: 4).

Epidural hematoma and subarachnoid hemorrhage groups were not included in the study because epidural hematoma case number was relatively small and subarachnoid hemorrhage could not be detected by DWI.

MRI imaging technique

A 1.5 Tesla system (Siemens Magnetom Symphony, Siemens, Erlangen, Germany) with phase arrayed head coil was used for detecting hematomas. Superconductor (Niobium-Titanium) magnets had a gradient strength of 30 mT/m.

A multislice axial plane with a singleshot, echoplanar spin echo sequence (b:500 sec/mm², 1000 sec/mm² and ADC) technique was performed for the evaluation. Axial DWI, TSE T2, SE T1 and FLAIR images and sagittal TSE T2 images were obtained. The MRI imaging parameters are demonstrated in Table 1.

Assesment of the images

All MR images were also transferred to an independent Workstation (Leonardo syngo 2002B, Siemens Ag Medical Solutions, Erlangen, Germany). The signal intensity changes of hematomas were determined by visual analysis of ADC maps and trace DWI (b=1000 sec/mm²) and also compared with normal white matter of contralateral cerebral hemisphere.

Table 1. Imaging parameters

| | DWI | TSE T2 Axial | SE T1 | FLAIR | TSE T2 Sagittal |
|------------------|---------|-----------------|---------|---------|--------------------|
| TR | 3900 | 3500 | 490 | 8000 | 4240 |
| TE | 107 | 90 | 9.4 | 105 | 107 |
| TI | - | - | - | 2600 | - |
| Slice thickness | 5.5 mm | 5.5 mm | 5.5 mm | 5.5 mm | 5 mm |
| Interval | 1 mm | 1 mm | 1 mm | 1 mm | 1 mm |
| Average | 2 | 2 | 2 | 1 | 2 |
| Matrix | 128x128 | 134x256 | 134x256 | 144x256 | 182x256 |
| FOV | 230 mm | 220 mm | 220 mm | 220 mm | 220 mm |
| Scan time | 52 sec | 96 sec | 103 sec | 130 sec | 125 sec |
| Number of slices | 20 | 21 | 21 | 21 | 21 |
| Slice gap | 15% | 20% | 20% | 20% | 20% |
| Bandwidth | 1346 | 100 | 139 | 139 | 195 |

Table 2. Scores of the intracerebral hematomas according to their signal characteristics on DWI and ADC maps. The intensity of the lesions were described according to the normal appearing white matter on the same side

| Stage | n | DWI | ADC maps | Point |
|----------------|----|--------------------------------------|---|-------|
| Hyperacute | 3 | Hyperintense | Hypointense | 1 |
| Acute | 5 | Hypointense | Hypointense | 2 |
| Early subacute | 10 | Hypointense | Hypointense | 2 |
| Late subacute | 9 | Hyperintense | Hypointense | 1 |
| Chronic | 6 | Peripheral hypo/Central hyperintense | Peripheral hypo/Central iso-hypointense | 3 |
| | 2 | Hypointense | Hypointense | 2 |

Table 3. Scores of the subdural hematomas according to their signal characteristics on DWI and ADC maps. The intensity of the lesions were described according to the normal appearing white matter on the same side

| Stage | n | DWI | ADC | Point |
|----------------|---|--------------|--------------|-------|
| Acute | 2 | Hypointense | Hypointense | 2 |
| Early subacute | 4 | Hypointense | Hypointense | 2 |
| Late subacute | 8 | Hyperintense | Hypointense | 1 |
| Chronic | 4 | Hypointense | Hyperintense | 4 |

Kruskal-Wallis test was performed for determining the differences between intracerebral and subdural hematomas by evaluating signal characteristics.

Because primary aim of our study was to determine the signal intensity characteristics of hematomas on DWI and ADC maps, we evaluated all groups and subgroups. For the determination of signal characteristic differences and expression of their contribution to the diagnosis, different phases of groups were compared with each other.

For the assesment of detectability of intracranial hematomas on DWI, conventional MRI sequences were accepted as a gold standart for intracerebral and subdural hematomas.

Statistical Analysis

Scores were given to intracerebral and subdural heatomas according to points compatible with different signal characteristics on DWI and ADC maps (Tables 2, 3).

3. Results

All intracerebral hematomas deteted on conventional MRI sequences were also detected on DWI.

All of the three hyperacute intracerebral hematomas were hyperintense on DWI and hypointense on ADC maps (Figure 1).

All the five acute and 10 subacute intracerebral hematomas were markedly hypointense on both DWI and ADC maps (Figure 2, 3).

Eight of the nine late subacute intracerebral hematomas were hyperintense on DWI and hypointense on ADC maps. One late subacute intracerebral hematoma was heterogenous hyperintense on DWI (Figure 4).

Six of the eight intracerebral chronic hematomas had a hyperintense center and a hypointense peripheral rim on DWI. On ADC maps, lesions had iso- to mildly hypointense center and a hiypointense rim which were interrupted in most cases. The other two ones were markedly hypointense on both DWI and ADC maps (Figures 5, 6).

All the subdural hematomas which were detected on conventional MRI sequences were also detected on DWI (Figure 7).

All two acute and four subacute hematomas were markedly hypointense on both DWI and ADC maps (Figure 8).

All of the eight late subacute subdural hematomas were hyperintense on DWI, six of them were hypointense and two other ones were iso- to mildly hypointense on ADC maps (Figure 9).

All of the four chronic subdural hematomas were hypointense on DWI and hyperintense on ADC maps (Figure 10).

None of the subarachnoid hemorrhages detected on CT was demonstrated on DWI (Figure 11).

Kruskal-Wallis test was performed for differentiation of hematoma phases according to scoring. As a result, it is found that it can offer a complete discrimination between hyperacute-late subacute phases and the other phases and between chronic phase and hyperacute-late subacute phases, and also a close discrimination between chronic phase and acute-early subacute phases for intracerebral hematomas. Such a discrimination between hyperacute and late subacute also between acute and early subacute-partially subacute phases could not be demonstrated. But for subdural hematomas acute-early subacute phase could be differentiated from late subacute-chronic phase and late subacute and chronic phases could be differentiated from the other phases (Table 4).

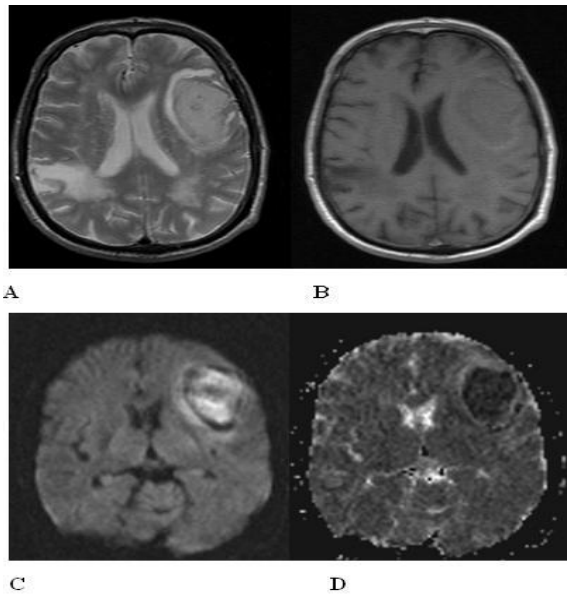


Fig. 1 (A-D): MR images of hyperacute intracerebral hematoma in a 72 years old male 12 hours after onset of symptoms. Hematoma in left frontal lobe is hyperintense on T2 weighted image (A) and hypo-to isointense on T1 weighted image (B). Peripheral hypointense rim is seen (more evident in the anterior of the lesion) in both T1 and T2 weighted images. On DWI (C) the center of hematoma is markedly hyperintense with patchy hypointense areas and a peripheral hypointense thin rim. These hypointense areas and hypointense rim are due to the magnetic susceptibility effects of deoxyhemoglobin.

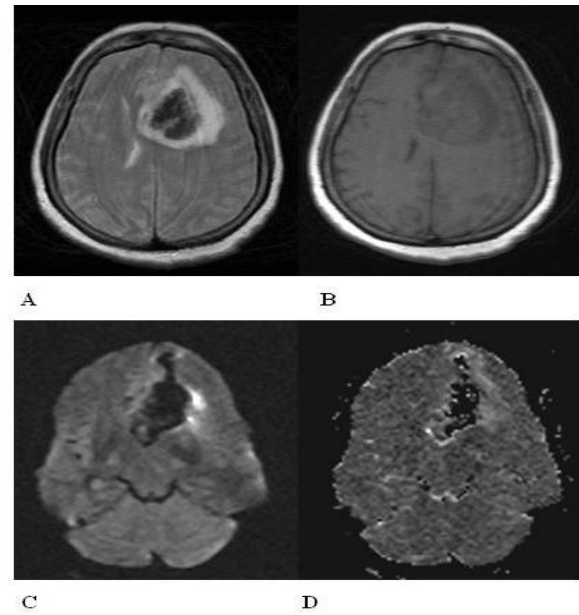


Fig. 2 (A-D): MR images of acute intracerebral hematoma in a 60 years old female 2 days after onset of symptoms. Hematoma in the left frontal lobe is markedly hypointense on T2 weighted image (A) and hypointense on T1 weighted image (B). Perilesional edema is also seen. Hematoma is markedly hypointense on both DWI (C) and ADC maps (D). The marked hypointensity seen on T2, DWI and ADC maps is due to the magnetic susceptibility artefacts of deoxyhemoglobin.

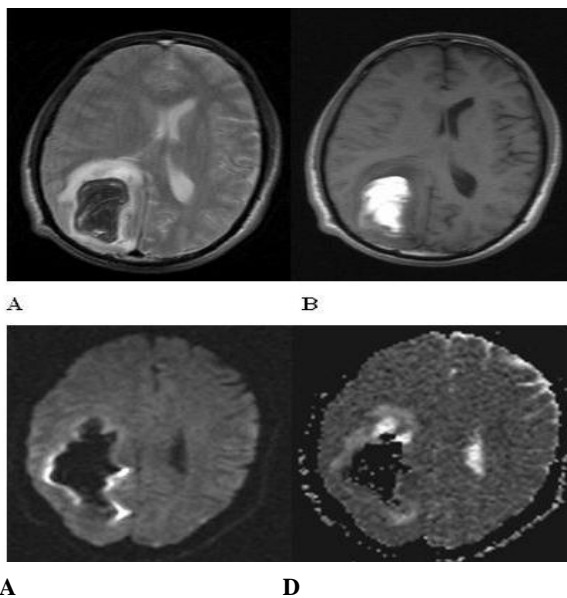


Fig. 3 (A-D): MR images of early subacute intracerebral hematoma in the 57 years old male 5 days after onset of symptoms. A right parieto-occipital hematoma is markedly hypointense on T2 weighted image (A) and hyperintense on T1 weighted image (B). Perilesional edema is also seen. Hematoma is markedly hypointense on both DWI and ADC maps. The marked hypointensity seen on T2, DWI and ADC maps is due to the magnetic susceptibility artefacts of deoxyhemoglobin.

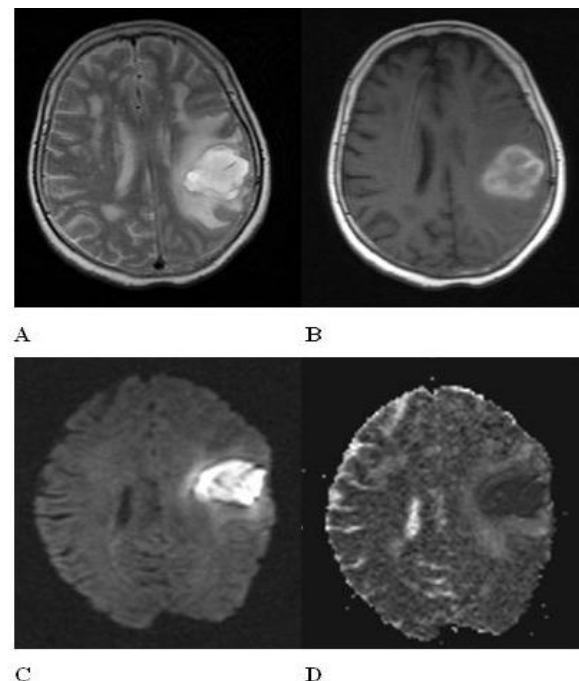
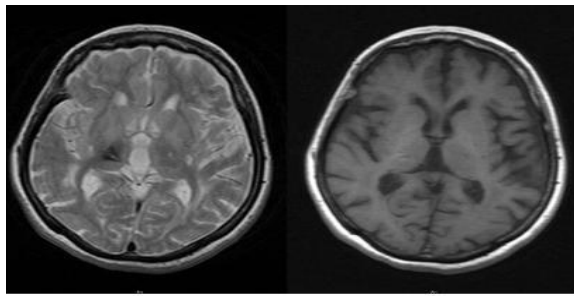
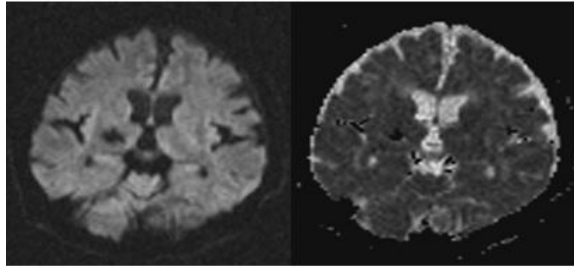


Fig. 4 (A-D): MR images of late subacute intracerebral hematoma in a 69 years old male 12 days after onset of symptoms. A left parietal hematoma is seen hyperintense on T2 weighted image (A) and heterogenous hyperintense on T1 weighted image (B). Hematoma is hyperintense on DWI (C) and hypointense on ADC maps (D). Perilesional edema is also seen.

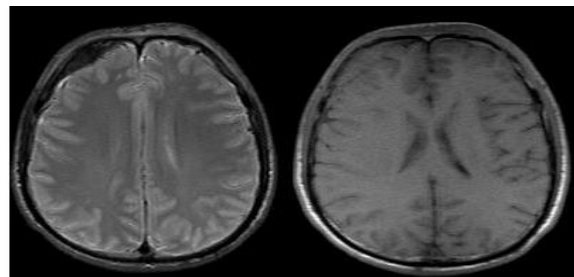


A B

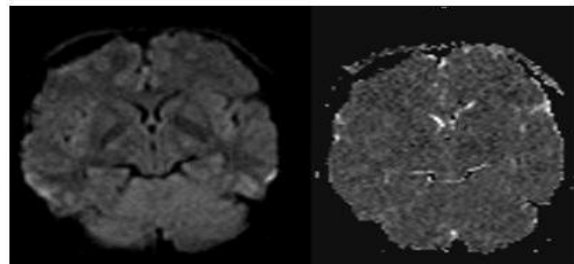


C D

Fig. 5 (A-D): Fifty-seven years old hypertensive female who was treated for intracerebral hematoma previously. MR images of chronic intracerebral hematoma 2 years after onset of symptoms. A hypointense area is seen due to hemosiderin deposits in right thalamus on T2 weighted image (A) which is iso-to mildly hypointense on T1 weighted image (B). Hematoma is markedly hypointense on both DWI (C) and ADC maps (D) due to magnetic susceptibility artefacts of hemosiderin.

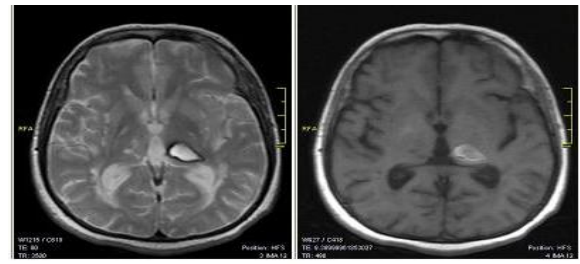


A B

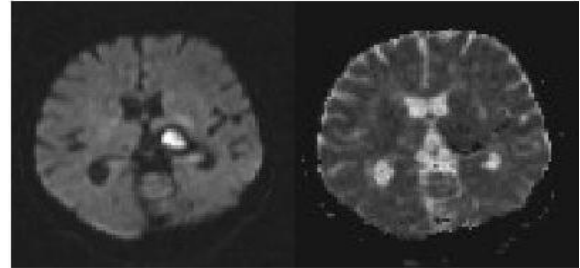


C D

Fig. 7 (A-D): Twenty-five years old male who has a right frontal subdural hematoma due to a blunt trauma. MR images of acute subdural hematoma is seen 1 day after trauma. Acute right frontal subdural hematoma is hypointense relative to white matter on T2 weighted images (A) and isointense on T1 weighted images (B). Subdural hematoma is markedly hypointense on both DWI (C) and ADC maps (D).

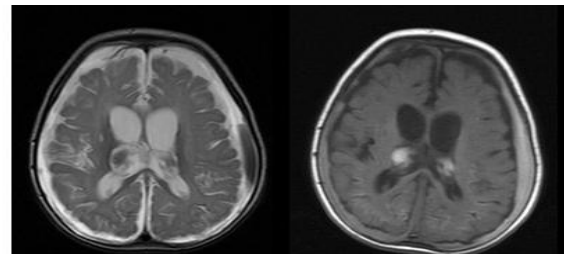


A B

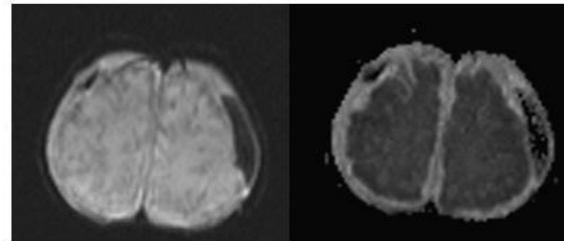


C D

Fig. 6 (A-D): Thirty years old hypertensive female who was treated for intracerebral hematoma previously. MR images of chronic intracerebral hematoma 57 days after onset of symptoms. A left thalamic hematoma has hyperintense center and a peripheral hypointense rim on T2 weighted images (A). The lesion is heterogenous iso-hyperintense on T1 weighted images (B). On DWI the center of the hematoma is hyperintense and there is a peripheral markedly hypointense rim (C). The center of the hematoma is iso-to mildly hypointense and also an incomplete ring-shaped hypointensity is seen on ADC maps (D).



A B



C D

Fig. 8 (A-D): Twenty-one years old female with cerebral palsy who has bleeding diathesis. She was treated for bilateral subdural hematoma previously. MR images of left parietal early subacute subdural hematoma 5 days after onset of symptoms which is hypointense relative to white matter on T2 weighted images (A) and hyperintense on T1 weighted images (B). Subdural hematoma is markedly hypointense on both DWI (C) and ADC maps (D).

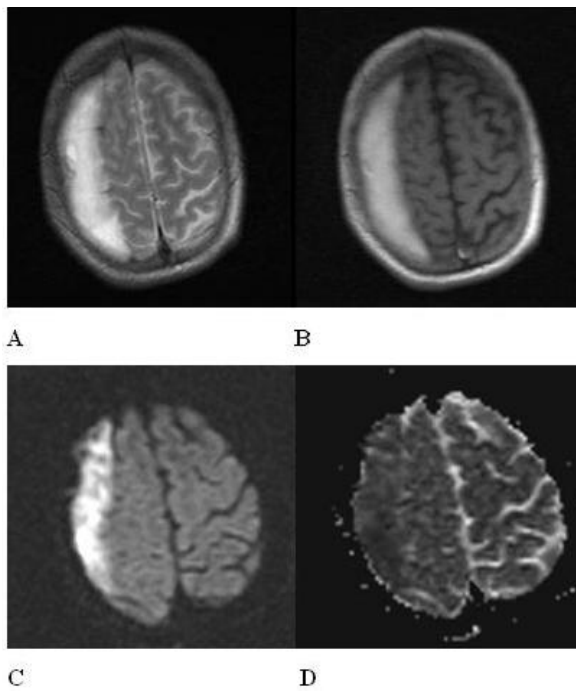


Fig. 9 (A-D): Thirty years old male who has a right frontoparietal subdural hematoma due to a blunt trauma. MR images of late subacute subdural hematoma 17 days after trauma is hypointense relative to white matter on both T2 (A) and T1 weighted images (B). Subdural hematoma is hyperintense on DWI(C) and hypointense on ADC maps.

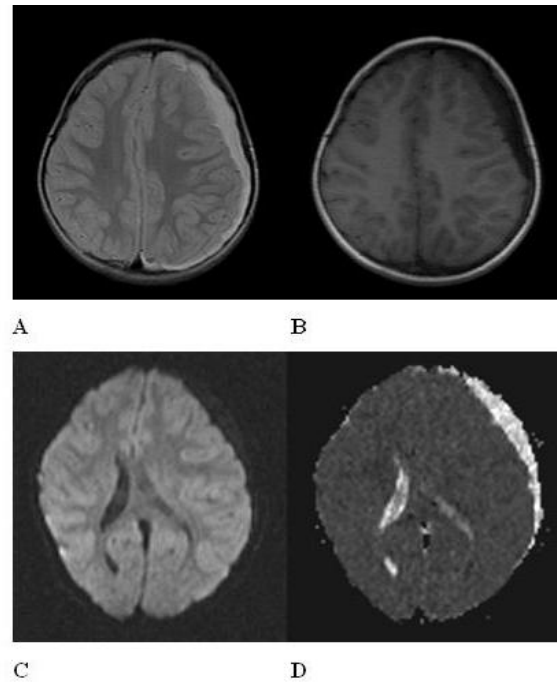


Fig. 10 (A-D): Nineteen years old male who has a left frontoparietal chronic subdural hematoma due to a blunt trauma. MR images are seen 3 months after trauma. The hematoma is hyperintense relative to white matter on T2 weighted images (A) and hypointense on T1 weighted images (B). The hematoma is hypointense on DWI (C) and hyperintense on ADC maps.

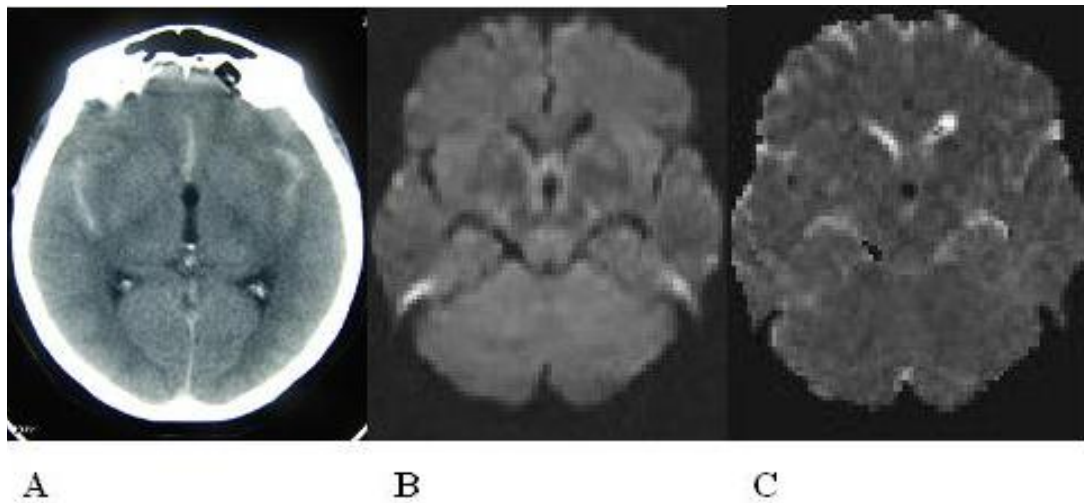


Fig. 11 (A-C): Fifty years old female who has a subarachnoid hemorrhage in bilateral sylvian fissures due to a blunt trauma which was detected on CT. MR images of subarachnoid hemorrhage are seen 3 days after trauma. On CT, there are linear high density areas in bilateral sylvian fissures (A). There is no any signal intensity changes in bilateral sylvian fissures on both DWI (B) and ADC maps (C).

Table 4. Signal characteristics of intracerebral and subdural hematomas on DWI

| | Intracerebral hematoma | | Subdural Hematoma | |
|----------------------|------------------------|--------------------|-------------------|--------------------|
| | DWI | ADC | DWI | ADC |
| Hyperacute phase | Hyperintense | Hypointense | - | - |
| Acute phase | Marked Hypointense | Marked Hypointense | Hypointense | Hypointense |
| Early subacute phase | Marked Hypointense | Marked Hypointense | Hypointense | Hypointense |
| Late subacute phase | Hyperintense | Hypointense | Hyperintense | Iso-to hypointense |
| Chronic phase | Variable | Variable | Hypointense | Hyperintense |

In addition, it has been suggested that acute hematoma could not be differentiated from subacute hematoma. A value $p < 0.05$ was considered statistically significant.

4. Discussion

Diffusion refers to the random microscopic translational motion of water molecules. It is known as a sensitive parameter for molecular tissue characterization (7).

Many clinical conditions, especially suspicion of stroke require DWI. It has been an important imaging method for evaluating tissue viability in early diagnosis and treatment of patients with acute cerebral ischemia (4,8). Before initializing the thrombolytic therapy and other interventions especially for the intracerebral hemorrhage, accurate differentiation of ischemic stroke from non-ischemic stroke is necessary.

Dorenbeck et al. (9) reported that intracerebral hemorrhagic lesions could show different signal intensities on DWI and ADC maps and they suggested some factors affecting diffusion in intracranial hemorrhage and hemorrhagic lesions. These factors are:

1. Susceptibility artefacts due to various entegration of bleeding products.
2. The shrinkage of extracellular space resulting from plasma resorption with clot retraction.
3. Membrane stability of red blood cells.

Hyperacute intracerebral hematoma

Kang et al. (2) (in all of their 6 patients) and Atlas et al. (10) reported (in all of their 3 patients) hyperintense center of hematoma and a surrounding hypointense peripheral rim in their patients with hyperacute intracerebral hematoma. Also we found similar signal intensities of hyperacute intracerebral hematomas with previous studies in our all 3 patients.

It is well known that hyperacute hematoma has a hyperintense center and a peripheral hypointense rim on T2 weighted images (11,12). On T2 weighted images central hyperintensity is attributed to intracellular oxyhemoglobin while hypointense rim is attributed to intracellular

deoxyhemoglobin. It is reported that this hypointense rim consists within several hours (12).

Oxyhemoglobin is hyperintense on DWI. Its ADC values are lower than normal brain parenchyma. This suggests that restricted water diffusion are inside red blood cells. The biophysical data of lower ADC values at the center of hyperacute hematoma is not clear. A probable cause is the shrinkage of extracellular space due to clot retractions with plasma resorption that leads to increased viscosity (11-14). The other probable explanation is contraction of red blood cells with decreased intracellular space and changes in molecular conformation of hemoglobin (10,15). Previous studies suggested that the reason of hypointensity of hyperacute hematoma seen on T2 weighted images was early formation of deoxyhemoglobin which had magnetic susceptibility effect (16-18). The hypointense rim on DWI is also seen on T2 weighted images consistently.

Acute and early subacute intracerebral hematoma

Does et al. (3) and Schafer et al. (4) reported that magnetic susceptibility effects lead to a decrease in ADC values and an accurate ADC value could not be surely calculated for acute and early subacute hamatomas. Similarly, Kang et al. (2) showed decreased ADC values at the center of early acute and subacute hematoma when compared with contralateral normal brain parenchyma. The most important two factors that cause these signal intensity patterns are identified as hemoglobin-oxygen status and accompanied presence of intact cells that compartmentalize paramagnetic material and paramagnetic iron. In addition they defined markedly hyperintense rims in all patients with hyperacute, acute, and subacute hematomas on DWI. Wiesmann et al. (18) suggested susceptibility artefacts as a probable cause of hyperintense rims surrounding

acute or subacute hematomas. Although Kang et al. (2) reported that this hypointense rim formation was not a result of a susceptibility artefact caused by paramagnetic material such as intracellular deoxyhemoglobin or methemoglobin but may be due to vasogenic edema which leads to T2 shine-through effects.

In our study, all of the acute and early subacute hematomas were markedly hypointense on DWI and ADC maps. This hypointensity in the hematomas occurs as a result of magnetic susceptibility artefact that is due to presence of intracellular deoxyhemoglobin or methemoglobin.

Late subacute intracerebral hematoma

Atlas et al. (10) reported that ADC values of late subacute hematoma are higher than normal white matter and the lysis of red blood cells leads to increased molecular diffusion.

Schaefer et al. (4) suggested that the ADC value of extracellular methemoglobin is higher than normal brain parenchyma and this difference is due to mobility of liquids in extracellular space.

Ebisu et al. (19) and Kang et al. (2) showed that late subacute hematoma was hyperintense on DWI while it had a lower signal intensity than normal white matter on ADC maps. In our study all of the subacute hematomas were hyperintense on DWI and hypointense on ADC maps.

At late subacute hematoma phase red blood cell lysis occurs and compartmentalization of methemoglobin disappears. Also intracellular contents spread to extracellular space leading increased viscosity. The other biological change in this phase is hypercellularity that is due to the infiltration of inflammatory cells and macrophages. All these changes can effect molecular diffusion of hematoma (20-22).

Chronic intracerebral hematoma

After a while, methemoglobin resorbs or precipitates and signal intensity of hematoma on T1 weighted images decreases. Higher water content leads to elongated T1-T2 relaxation times. From the beginning of hemorrhage, hemoglobin is phagocytized continuously. Hemoglobin products ferritin and hemosiderin persists in phagocytic cells that are indicators of an old hemorrhage which is located at the periphery of hematoma (20,23).

Hemosiderin and ferritin cause magnetic susceptibility artefacts which are seen predominantly on T2 weighted images (20,21,23). Chronic hematomas are hyperintense on DWI (2,4). But older chronic hematomas may exhibit hypointense signal characteristics (24). An

accurate calculation on DWI is difficult because of the peripheral deposits of hemosiderin and ferritin (3,23).

In a study of Kang et al. (2) including eight late chronic phase hematoma patients, they reported that hematomas were markedly homogenous hypointense in four patients while demonstrating a isointense center with a hypointense surrounding rim in the other four patients. They suggested that a center of a lesion which started a cystic evolution is seen isointense at early chronic phase and hypointense on late chronic phase on DWI. They proposed that these signal intensity changes were not due to status of red blood cell membranes.

Ebisu et al. (19) reported that the center of intracellular haemorrhage tends to have a low ADC value in the chronic phase.

Schaefer et al. (4) demonstrated that, chronic intracerebral hematoma is hypointense on DWI and its ADC values can not be calculated accurately.

In our study, in 6 of 8 patients with chronic intracerebral hematoma, (range between 33 days-5 months) lesions had hyperintense center and a marked peripheral hypointense rim that was due to a hemosiderin rim causing magnetic susceptibility artefacts. While the center of lesion was iso- to mildly hypointense, there was a marked peripheral hypointense rim on ADC maps. Also hematomas were hyperintense on T1 weighted images in all these patients. We believe that, extracellular methemoglobin persists for an extended period in chronic hematoma and is responsible for high signal intensity at the center of the lesion.

In our study, in 2 of 8 patients with chronic intracerebral hematoma (period range between 15 months-2 years), hematomas were resorbed and markedly hypointense on DWI and ADC maps due to magnetic susceptibility artefacts of hemosiderin deposits. Our findings support the results of Schaefer et al (4).

Subdural hematoma

Lin et al. (5) compared the efficiency of GRE and DWI in patients with subdural hematoma and they detected all the lesions on b0 EPI.

In 29 of 31 patients with chronic subdural hematoma, Kuwahara et al. (25) demonstrated that lesions were hypointense on DWI because of free movement of water molecules rather than presence of extracellular methemoglobin. They confirmed that, expression of solid clots on DWI and calculation of the values on ADC maps were useful for the discrimination of liquid-solid compartments and could provide an appropriate

surgical treatment choice to the patients with traumatic subacute-subdural organised hematoma. Chronic subdural hematoma is classified into three groups according to their signal characteristics on DWI: Homogeneous, separate, and trabecular type. Homogeneous type is defined as homogenous hypointense hematoma. Separate type is described as a subdural hematoma that has two contents with different signal intensities. Trabecular type is referred to a multiloculated hematoma with a septation lying between inner and outer membranes. Also they observed a high intensity line or a crescent along the membranes and this was termed as subdural hyperintense band.

Because hyperacute phase is within three hours from the bleeding onset and clinical manifestations are not so noticeable in this period, we have no any MR images for hyperacute phase. We did not include hyperacute hematomas in our study because we did not have any patient in this phase. Two acute subdural and four early subacute hematomas were markedly hypointense on both DWI and ADC maps. Similar to intracerebral paraneural hematomas, we think that this hypointensity is due to magnetic susceptibility effects of paramagnetic intracellular deoxyhemoglobin and methemoglobin in early and subacute hematomas.

All of the eight late subacute hematomas were hyperintense on DWI while six of them were hypointense and the other two were isohypointense on ADC maps. The factors which maintain signal intensity characteristics of the hematoma in this phase may be shrinkage of the extracellular space due to extravasated methemoglobin from red blood cell lysis and presence of extracellular methemoglobin.

All of the four chronic subdural hematomas were hypointense on DWI and hyperintense on ADC maps. Similarly to Kuwahara et al. (25) we suggest that the hypointensity of the chronic subdural hematoma on DWI is due to free water molecule movements. We did not observe a subdural hyperintense band in any of our patients which Kuwahara et al. (25) detected in their study. Also all of the chronic hematomas were hypointense on DWI.

Signal characteristics of subdural hematoma on DWI are not well established. In literature except from a limited data about some phases, there is no any study that assesses subdural hematomas findings on DWI according to their phases.

Subarachnoid hemorrhage

CT is still the most important imaging modality for detecting acute subarachnoid hemorrhage. But

many studies suggest that FLAIR MRI sequence is more sensitive for detecting especially older subarachnoid hemorrhage which can not be seen on CT. CSF dilutes subarachnoid hemorrhage, resulting in a decreased hematocrit. The potential reasons that affect intensity characteristics of subarachnoid hemorrhage on DWI are shrinkage of extracellular space due to clot retraction, changes in the osmolarity of extracellular blood, fibrin web formation associated with clot presence, T2 shine through effect, decreased local cell volume, high protein density, and increased viscosity (26).

Lin et al. (5) compared GRE and DWI for detecting subarachnoid hemorrhage in four patients and they established the subarachnoid hemorrhage in two of them on GRE while none of them was detected on b0 EPI.

Wiesmann et al. (27) reported that subarachnoid hemorrhage could be detected with FLAIR and proton density images while it could not be demonstrated with T2 and DWI.

On DWI, Shimoda et al. (6) detected the hemorrhage in 34 of 72 patients with subarachnoid hemorrhage. They emphasized that the subarachnoid hemorrhages they detected were relatively larger and the detection of subarachnoid hemorrhages by DWI was strongly correlated with hemorrhage volume and clot density.

We did not detect any hemorrhage by DWI in our 12 patients with subarachnoid hemorrhage which were detected by CT. One probable reason for this seems to be relative small volume of subarachnoid hemorrhage in these cases.

5. Conclusion

All the intracerebral and subdural hematomas which were seen on conventional MRI sequences can also be detected on DWI. DWI is not a sensitive imaging modality for detecting subarachnoid hemorrhage.

Intracerebral hematomas are markedly hypointense on DWI because of magnetic susceptibility effects of hemosiderin, intracellular deoxyhemoglobin and methemoglobin. Thus all of acute and early subacute hematomas and some of the chronic hematomas have similar signal intensity characteristics on DWI.

Also hyperacute and late subacute hematomas have similar signal intensity characteristics. Age of hematoma and volume of hematoma after resorption are the most important factors affecting signal intensity of chronic hematomas and their signal intensities on DWI may exhibit some differences.

The signal intensities of acute and early subacute subdural hematomas on DWI are similar. Because of the hyperacute phase was excluded from this study due to some limitations, and there is no adequate data about this phase we do not present results about similarities and differences of this phase with the other phases. Thus it seems impossible to demonstrate phases of subdural hematomas accurately by only DWI.

Except from chronic subdural hematomas that were detected on DWI, signal characteristics of all of the intracranial hematomas were similar to their T2 signal intensities and also they were hypointense on ADC maps.

In conclusion we think that DWI can only provide limited data and can not give definite results for determining phases of intracranial hematomas. The lesions should also be assessed with other conventional MRI sequences.

References

1. Tsuruda JS, Chew WM, Moseley ME, Norman D. Diffusion-weighted MR imaging of the brain: value of differentiating between extraaxial cysts and epidermoid tumors. *AJNR Am J Neuroradiol* 1990; 11: 925-931.
2. Kang BK, Na DG, Ryoo JW, et al. Diffusion-weighted MR imaging of intracerebral hemorrhage. *Korean J Radiol* 2001; 2: 183-191.
3. Does MD, Zhong J, Gore JC. In vivo measurement of ADC change due to intravascular susceptibility variation. *Magn Reson Med* 1999; 41: 236-240.
4. González RG, Schaefer PW, Buonanno FS, et al. Diffusion-weighted MR imaging: diagnostic accuracy in patients imaged within 6 hours of stroke symptom onset. *Radiology* 1999; 210: 155-162.
5. Lin DD, Filippi CG, Steever AB, Zimmerman RD. Detection of intracranial hemorrhage: comparison between gradient-echo images and b(0) images obtained from diffusion-weighted echo-planar sequences. *AJNR Am J Neuroradiol* 2001; 22: 1275-1281.
6. Shimoda M, Hoshikawa K, Shiramizu H, et al. Clinical implications of subarachnoid clots detected by diffusion-weighted imaging in the acute stage of aneurysm rupture. *Neurol Med Chir (Tokyo)* 2010; 50: 192-199.
7. Le Bihan D, Turner R, Douek P, Patronas N. Diffusion MR imaging: clinical applications. *AJR Am J Roentgenol* 1992; 159: 591-599.
8. Sunshine JL, Tarr RW, Lanzieri CF, et al. Hyperacute stroke: ultrafast MR imaging to triage patients prior to therapy. *Radiology* 1999; 212: 325-332.
9. Dorenbeck U, Schlaier J, Bretschneider T, Schuierer G, Feuerbach S. Diffusion-weighted imaging with calculated apparent diffusion coefficient in intracranial hemorrhagic lesions. *Clin Imaging* 2005; 29: 86-93.
10. Atlas SW, DuBois P, Singer MB, Lu D. Diffusion measurements in intracranial hematomas: implications for MR imaging of acute stroke. *AJNR Am J Neuroradiol* 2000; 21: 1190-1194.
11. Linfante I, Llinas RH, Caplan LR, Warach S. MRI features of intracerebral hemorrhage within 2 hours from symptom onset. *Stroke* 1999; 30: 2263-2267.
12. Clark RA, Watanabe AT, Bradley WG Jr, Roberts JD. Acute hematomas: effects of deoxygenation, hematocrit, and fibrin-clot formation and retraction on T2 shortening. *Radiology* 1990; 175: 201-206.
13. Hayman LA, Taber KH, Ford JJ, et al. Effect of clot formation and retraction on spin-echo MR images of blood: an in vitro study. *AJNR Am J Neuroradiol* 1989; 10: 1155-1158.
14. Hayman LA, Ford JJ, Taber KH, et al. T2 effect of hemoglobin concentration: assessment with in vitro MR spectroscopy. *Radiology* 1988; 168: 489-491.
15. Hargens AR, Bowie LJ, Lent D, et al. Sick-cell hemoglobin: fall in osmotic pressure upon deoxygenation. *Proc Natl Acad Sci USA* 1980; 77: 4310-4312.
16. Schellinger PD, Jansen O, Fiebich JB, Hacke W, Sartor K. A standardized MRI stroke protocol: comparison with CT in hyperacute intracerebral hemorrhage. *Stroke* 1999; 30: 765-768.
17. Felber S, Auer A, Wolf C, et al. [MRI characteristics of spontaneous intracerebral hemorrhage]. [Article in German] *Radiologe* 1999; 39: 838-846.
18. Wiesmann M, Mayer TE, Yousry I, Hamann GF, Brückmann H. Detection of hyperacute parenchymal hemorrhage of the brain using echo-planar T2*-weighted and diffusion-weighted MRI. *Eur Radiol* 2001; 11: 849-853.
19. Ebisu T, Tanaka C, Umeda M, et al. Hemorrhagic and nonhemorrhagic stroke: diagnosis with diffusion-weighted and T2-weighted echo-planar MR imaging. *Radiology* 1997; 203: 823-828.
20. Gomori JM, Grossman RI, Goldberg HI, Zimmerman RA, Bilaniuk LT. Intracranial hematomas: imaging by high-field MR. *Radiology* 1985; 157: 87-93.
21. Bradley WG Jr. MR appearance of hemorrhage in the brain. *Radiology* 1993; 189: 15-26.
22. Brooks RA, Di Chiro G, Patronas N. MR imaging of cerebral hematomas at different field strengths: theory and applications. *J Comput Assist Tomogr* 1989; 13: 194-206.
23. Ekholm S. Intracranial hemorrhages. *Rivista di Neuroradiologia* 1996; 9: 17-21.
24. Moritani T, Ekholm S, Westesson P. Editors, *DW imaging of Brain*, Springer Berlin Heidelberg New York Business. 2005; 80-81.
25. Kuwahara S, Fukuoka M, Koan Y, et al. Subdural hyperintense band on diffusion-weighted imaging of chronic subdural hematoma indicates bleeding from the outer membrane. *Neurol Med Chir (Tokyo)* 2005; 45: 125-131.
26. Noguchi K, Ogawa T, Seto H, et al. Subacute and chronic subarachnoid hemorrhage: diagnosis with fluid-attenuated inversion-recovery MR imaging. *Radiology* 1997; 203: 257-262.
27. Wiesmann M, Mayer TE, Yousry I, et al. Detection of hyperacute subarachnoid hemorrhage of the brain by using magnetic resonance imaging. *J Neurosurg* 2002; 96: 684-689.